



CRBGP Inhibited The Activity of Glioma U251 Cells Through Suppressing FAK-AKT Pathway and The Secretion of Interleukin-6*

HAN Jian-Mei, LI Jia-Yang, BA Yue, ZHOU Rong, LI Shuang-Jiao, XIAO Rong**

(School of Life Science, Liaoning Normal University, Dalian 116081, China)

Abstract Objective Voltage-gated sodium channels (VGSCs) are expressed in glioma U251 cells and affect the proliferation, invasion and apoptosis of U251 cells. It is reasonable to hypothesize that the cysteine-rich buccal gland protein (CRBGP), a VGSCs blocker isolated from the buccal glands of *Lampetra japonica*, may suppress the activity of U251 cells. **Methods** Firstly, the proliferation of U251 cells in the presence of CRBGP was detected by MTT assay. And the morphology, cytoskeleton and nucleus of U251 cells after treated with CRBGP were observed by Wright-Giemsa, FITC-phalloidin and Hoechst 33258 staining assays, respectively. Subsequently, extracellular matrix proteins such as collagen IV, fibronectin and laminin were used to detect the effect of CRBGP on U251 cells' adhesion. In addition, the migration and invasion of U251 cells treated with CRBGP were detected by transwell assays. And the internal mechanisms of CRBGP on U251 cells' apoptosis and mobility were explored by Western blot. Finally, the anti-inflammatory effect of CRBGP on U251 cells was detected by enzyme linked immunosorbent assay. **Results** CRBGP inhibited the proliferation of U251 cells by inducing apoptosis in a mitochondrial-dependent pathway and preventing the release of proinflammatory factor interleukin-6. Also, the VGSCs blocking and anti-inflammatory activities of CRBGP contributed to its inhibitory effects on the adhesion, migration and invasion of U251 cells. Finally, CRBGP affected the proliferation and mobility of U251 cells through the suppression of the FAK-AKT pathway. **Conclusion** Together, our data indicated that CRBGP could exhibit its anti-tumor activity probably by its VGSCs inhibitory property, providing a basis for the functional information of VGSCs to the gliomas.

Key words gliomas, U251 cells, VGSCs, CRBGP, IL-6

DOI: 10.16476/j.pibb.2021.0359

Human gliomas represent a group of tumors that are derived from the glial cells in the brain^[1]. According to the different clinical features, gliomas were classified into four grades by the World Health Organization (WHO), including the low-grade gliomas I and II, as well as the high-grade gliomas III and IV^[2]. Due to the relatively high infiltration, lots of patients with gliomas would suffer the metastatic tumors even after treatment with surgical resection, radiotherapy and chemotherapy^[3-5]. Thus, it is not surprising that the morbidity, recurrence and mortality of gliomas are usually very high^[6]. Recently, the incidence and mortality of gliomas increased worldwide especially in developing countries^[7]. Most importantly, the lifetime for high-grade glioma (IV) patients is usually no more than 14 months^[1]. Although great progress was made on gene mutations that are responsible for the development of gliomas,

the ambiguous mechanisms which lead to the formation of gliomas and their relatively high mortality still drive us to find more effective molecules and therapies to eliminate the pain and despair that originated from this malignant brain tumor^[8].

U251 cells are classic astrocytomas that were reported to express a variety of ion channels including voltage-gated sodium channels (VGSCs), chloride voltage-gated channel 3, transient receptor potential channels, and Ca²⁺-activated K⁺ channel KCa3.1^[9-12]. And these channels were observed to promote the abilities of U251 cells on migration and invasion^[9-12].

* This work was supported by grants from The National Natural Science Foundation of China (31301880) and Natural Science Foundation of Liaoning Province (20180550829).

** Corresponding author.

Tel: 86-411-85992862, E-mail: xiaorong_lnu@126.com

Received: November 23, 2021 Accepted: December 2, 2021

Thus, suppression of the activity of these channels might inhibit the high infiltration property of U251 cells. In our previous studies, a VGSCs inhibitor named cysteine-rich buccal gland protein (CRBGP) was reported to block the activity of endothelial cells (human umbilical vein endothelial cells, HUVECs) and cervical cancer cells (HeLa cells) as these two cell lines are also reported to express VGSCs^[13-18]. However, the detailed mechanisms need further study. Whether CRBGP could act on other tumor cell lines, *e. g.* astrocytoma U251 cells with higher infiltrative characterizations? In the present study, the suppressive roles of CRBGP on U251 cells were detected and the signaling pathway was dissected.

1 Materials and methods

1.1 Chemicals

3-(4,5-dimethylthiazol-2-yl)-2,5-diphenyltetrazolium bromide (MTT), dimethyl sulfoxide (DMSO), phosphate buffered saline (PBS), BeyoECL plus detection kit and other reagents were purchased from Solarbio (China). Bicinchoninic acid (BCA) assay kit and Hoechst 33258 were bought from Beyotime (China). Dulbecco's modified Eagle's medium (DMEM), fetal bovine serum (FBS), 0.25% trypsin-EDTA were purchased from Gibco (USA). Penicillin and streptomycin were purchased from Hyclone (USA). FITC-labeled phalloidin was purchased from Enzo Life Sciences (USA). Human collagen IV, fibronectin, and laminin were purchased from Sigma (USA). The polyvinylidene difluoride (PVDF) membranes were from Millipore (USA). Antibodies against B cell lymphoma 2 (BCL2), BCL2-associated X (BAX), Caspase 3, phosphorylated focal adhesion kinase (p-FAK), protein kinase B (PKB/AKT), phosphorylated PKB/AKT (p-PKB/p-AKT) and glyceraldehyde-3-phosphate dehydrogenase (GAPDH) were purchased from Proteintech (China). Human IL-6 ELISA kit was purchased from Westang (China).

1.2 Purification of CRBGP and culture of glioma U251 cells

According to Xiao's report^[19], the separation of CRBGP from lamphredin which was extracted from the buccal glands of *Lampetra japonica* (*L. japonica*) was performed by a sephadex G-75 column. The elution buffer which contained the purified CRBGP was firstly collected, dialysed with NH_4HCO_3 , and finally lyophilized with a vacuum freeze dryer

(Christ). After determination of the concentration with BCA assay kit, the purified protein was loaded on sodium dodecyl sulfate-polyacrylamide gel electrophoresis (SDS-PAGE). Human glioma cell line U251 cells were obtained from Dr. QIANG Min at ShanghaiTech University. The U251 cells were grown in DMEM containing 10% FBS and 1% penicillin/streptomycin at 37°C in a CO_2 incubator (Thermo Scientific).

1.3 Determination of cell proliferation

The proliferation of U251 cells was determined by MTT assay. Briefly, U251 cells were harvested with 0.25% trypsin-EDTA and then seeded (1×10^3 cells/well) in a 96-well plate. After growing at 37°C for 24 h, the U251 cells were washed with PBS and then incubated with FBS-free DMEM which contained PBS and CRBGP from 3 to 25 $\mu\text{mol/L}$ (3, 5, 7, 7.5, 9.8, 13, 20 and 25 $\mu\text{mol/L}$), respectively. 24 h later, MTT with a final concentration of 5 g/L (10 μl) was added directly to each well for an additional incubation at 37°C for 4 h. Subsequently, the above medium was carefully removed from the 96-well plate and DMSO (100 $\mu\text{l/well}$) was added to dissolve the formazan crystals formed in the live U251 cells. In order to dissolve the formazan crystals completely, the 96-well plate was agitated on a shaker at 100 r/min for 10 min. Finally, the absorbance of each well in the 96-well plate was measured at 492 nm with a microplate reader (Thermo Scientific). The U251 cells in the PBS group were set as a control group and their absorbance at 492 nm was set as 100%. The U251 cells' proliferation in the CRBGP (from 3 to 25 $\mu\text{mol/L}$) treated groups was calculated as described in our previous study^[14].

1.4 Morphologic observation

Firstly, U251 cells were seeded on the glass slides in 24-well plates for 24 h in the CO_2 incubator. Then, U251 cells were treated with PBS and CRBGP (6.5 and 13 $\mu\text{mol/L}$) for an additional incubation of 24 h, respectively. Next, the U251 cells on the glass slides in 24-well plates were fixed with 4% paraformaldehyde (PFA) at room temperature (RT) for 5 min. For Wright-Giemsa assay, the fixed U251 cells were incubated with a 200 μl staining agent for 15 min, washed with the sterilized water twice, and then captured with an inverted microscope (Nikon). For cytoskeleton and nucleus detection, the fixed U251 cells were firstly labeled with FITC-phalloidin (5 mg/L) for 30 min, and then labeled with Hoechst

33258 (1 mg/L) for 10 min in the dark room to prevent fluorescence from quenching. After washing the slides with PBS three times, the U251 cells treated with PBS and CRBGP (6.5 and 13 $\mu\text{mol/L}$) were visualized using laser scanning confocal microscopy (Carl Zeiss, 630 \times).

1.5 Western blot

The U251 cells cultured in a 6-well plate were treated with PBS and CRBGP (6.5 and 13 $\mu\text{mol/L}$) for 24 h in the CO_2 incubator. Subsequently, the PBS and CRBGP pretreated U251 cells were washed with PBS twice and then collected with lysis buffer which contains 50 mmol/L Tris-HCl (pH 7.4), 150 mmol/L NaCl, 1% Nonidet P-40, 0.5% sodium deoxycholate, and 0.1% SDS in the presence of 1% phenylmethanesulfonyl fluoride (PMSF) as protease inhibitor on ice for 10 min. The U251 cells' lysates were separated on 12% SDS-PAGE, transferred onto the PVDF membranes and then blocked with 5% defatted milk which was dissolved in Tris buffered saline tween (TBST) buffer (20 mmol/L Tris-HCl, pH 8.0, 150 mmol/L NaCl and 0.05% Tween-20) at 37°C for 1 h. Next, the membranes were respectively incubated with primary antibodies including BAX, BCL2, Caspase 3, p-FAK, AKT, p-AKT and GAPDH at the ratio of 1:500 overnight at 4°C. After washing with TBST buffer three times, the membranes were incubated with secondary antibodies (1:5000) at RT for 2 h. Finally, the membranes were washed with TBST buffer and then visualized on the FluorChem Q (Protein Simple) using BeyoECL plus detection kit. GAPDH was employed as a positive control. The level of the above proteins was analyzed by the FluorChem Q software, and calculated with the formula reported in our previous study^[14].

1.6 Analysis of U251 cells' adhesion, migration and invasion

In order to detect the effect of CRBGP on the adhesive ability of U251 cells, the extracellular matrix (ECM) proteins, such as collagen IV, fibronectin and laminin, were respectively added in a 96-well plate at 4°C overnight. After removing the residual ECM proteins, the PBS and CRBGP (6.5 and 13 $\mu\text{mol/L}$) pretreated U251 cells were respectively put into the above 96-well plate and incubated in the CO_2 incubator for 4 h. Subsequently, the non-adhesive U251 cells were washed with PBS twice, and the number of the adhesive U251 cells was measured by the MTT assay. In order to assay whether CRBGP

could affect the migratory and invasive abilities of the U251 cells, the PBS and CRBGP (6.5 and 13 $\mu\text{mol/L}$) pretreated U251 cells were cultured in DMEM in the absence of FBS and placed on the upper chambers of the transwell. Meanwhile, the chambers below the polycarbonate filter were full of DMEM supplemented with basic fibroblast growth factor (bFGF, 3 $\mu\text{g/L}$) and FBS (15%). After 20 h (migration assay) and 32 h (invasion assay), the non-migrated and non-invaded U251 cells were respectively removed from the polycarbonate filter using a cotton swab. And the migrated and invaded U251 cells on the polycarbonate filter were fixed with 4% PFA for 5 min, stained with Wright-Giemsa solution for 15 min and photographed by the inverted microscope (Nikon). In the present study, three parallel samples in each group including the PBS and CRBGP-treated U251 cells were performed, and three fields in each sample were randomly selected to count the number of the U251 cells, and calculate their average number in each group. Besides, the upper chambers of transwell in the invasion assay were precoated with the matrigel at 37°C for 20 min. The migratory and invasive abilities of U251 cells in the presence of CRBGP were analyzed by the method reported in our previous study^[14].

1.7 Detection of proinflammatory factor interleukin-6 (IL-6)

The U251 cells cultured in a 96-well plate were respectively treated with PBS and lipopolysaccharide (LPS) with a final concentration of 430 mg/L in the CO_2 incubator. After 5 h, PBS and CRBGP (6.5 and 13 $\mu\text{mol/L}$) were also added into the 96-well plate respectively. When the treatment reached 24 h, the supernatant of U251 cells was, respectively, collected into tubes for enzyme-linked immunosorbent assay (ELISA). The supernatant was respectively added into the wells which were pre-coated with mouse anti-human IL-6 antibody at 37°C for 2 h, followed by washing with PBS with Tween 20 (PBST) buffer five times. Subsequently, a biotinylated anti-human IL-6 antibody was added into each well at 37°C for 40 min. After washing with PBST buffer five times, horseradish peroxidase-labeled with streptavidin was added into the above wells and incubated at 37°C for 30 min, and then the plate was also washed with PBST buffer. Finally, the wells were incubated with 3',5',5'-tetramethylbenzidine (TMB) solution at 37°C for 15 min and detected at 450 nm with the microplate

reader. Furthermore, the absorbance at 450 nm of standard IL-6 at a series of concentrations was also detected with the microplate reader following the manufacturer's instructions.

1.8 Statistical analysis

All data were reported in the form of means \pm standard deviation (SD), and the experiments were carried out at least three times. The Student's *t*-tests were performed to compare the values of the PBS and CRBGP (6.5 and 13 $\mu\text{mol/L}$) treated groups ($*P < 0.05$; $**P < 0.01$ and $***P < 0.001$).

2 Results

2.1 The proliferation of glioma U251 cells was inhibited by CRBGP

The VGSCs inhibitor CRBGP was obtained with relatively higher purity according to our previous report (data not shown)^[19]. In addition to endothelial cells HUVECs and cervical cancer HeLa cells, glioma U251 cells were also reported to express high levels of VGSCs^[9]. As the VGSCs inhibitor CRBGP could effectively suppress the proliferation of both HUVECs and HeLa cells, the role of CRBGP on the proliferation of glioma U251 cells was examined in this study. U251 cells were treated with PBS and CRBGP ranging from 3 to 25 $\mu\text{mol/L}$ (3, 5, 7, 7.5, 9.8, 13, 20 and 25 $\mu\text{mol/L}$) for 24 h, respectively. As shown in Figure 1, CRBGP significantly inhibited the proliferation of glioma U251 cells in a concentration-

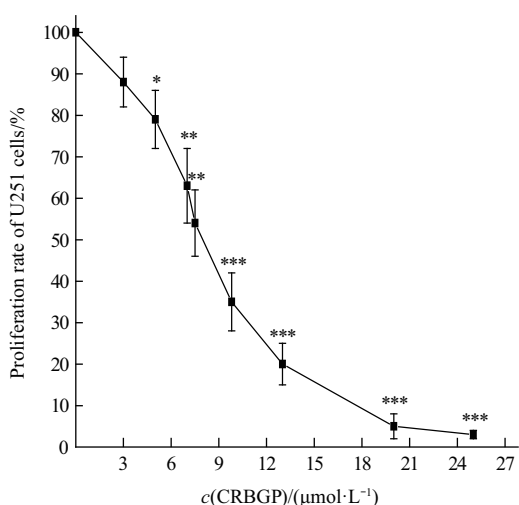


Fig. 1 CRBGP suppressed the proliferation of glioma U251 cells

The U251 cells were treated with PBS and various concentrations of CRBGP (3, 5, 7, 7.5, 9.8, 13, 20 and 25 $\mu\text{mol/L}$) at 37°C for 24 h. The significant differences were marked by asterisks ($*P < 0.05$; $**P < 0.01$; $***P < 0.001$).

dependent manner, compared with the PBS (control) group. And the half-maximal inhibitory concentration (IC_{50}) of CRBGP on U251 cells' proliferation was 8.3 $\mu\text{mol/L}$, which was a little higher than that on HeLa cells (6.7 $\mu\text{mol/L}$) and HUVECs (4 $\mu\text{mol/L}$)^[14,16]. Based on our MTT assay, 6.5 and 13 $\mu\text{mol/L}$ of CRBGP inhibited the proliferation rate of U251 cells by 30% (less than 50% of the proliferation rate) and 80% (higher than 50%), respectively. Therefore, we chose these two concentrations of CRBGP to treat the U251 cells for the following study.

2.2 The morphology of glioma U251 cells was altered by CRBGP

In addition to the inhibitory effect of CRBGP on the proliferation of U251 cells, CRBGP was also found to alter the morphology of U251 cells. According to Wright-Giemsa assay, not only the number of U251 cells was reduced in the CRBGP-treated groups, but also their size became smaller when compared with the PBS group (Figure 2). In addition, CRBGP reduced the junctions between U251 cells. After treating with CRBGP, the ectomas of U251 cells gradually vanished and the shape of U251 cells changed, from spindle to round (Figure 2, 3). Furthermore, more vacuole bodies were observed in CRBGP-treated U251 cells (Figure 3). As cytoskeleton was reported to cause the change of cell shape, F-actin which is the main component of cytoskeleton was labeled with FITC-phalloidin. As shown in Figure 3, F-actin (green signals) in the control U251 cells localized at the cytoskeleton around the cell membrane; the green signals gradually disappeared in the CRBGP-treated U251 cells. Compared with the controls, 6.5 and 13 $\mu\text{mol/L}$ CRBGP reduced the relative fluorescent intensity of phalloidin labeled with FITC to (48.4 \pm 14.4)% ($P < 0.01$) and (36.7 \pm 6.5)% ($P < 0.001$) respectively, which displayed the organization of F-actin. Besides the cytoskeleton, the nuclei of the U251 cells in the CRBGP groups also became smaller when compared with the control group (Figure 3).

2.3 The apoptosis of glioma U251 cells was induced by CRBGP

Hoechst 33258 staining assay showed the nuclei of the U251 cells became shrank in the 6.5 and 13 $\mu\text{mol/L}$ CRBGP-treated groups, indicating that CRBGP might induce apoptosis in U251 cells. In order to further investigate the intrinsic mechanism of apoptosis, the content of apoptosis-related proteins

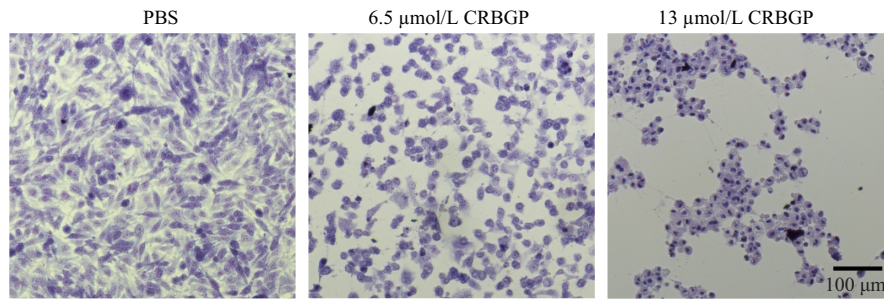


Fig. 2 CRBGP affected the morphology of glioma U251 cells

The U251 cells pretreated with PBS, 6.5 and 13 $\mu\text{mol/L}$ CRBGP were stained with Wright-Giemsa staining solution and observed by the invert microscope in brightfield.

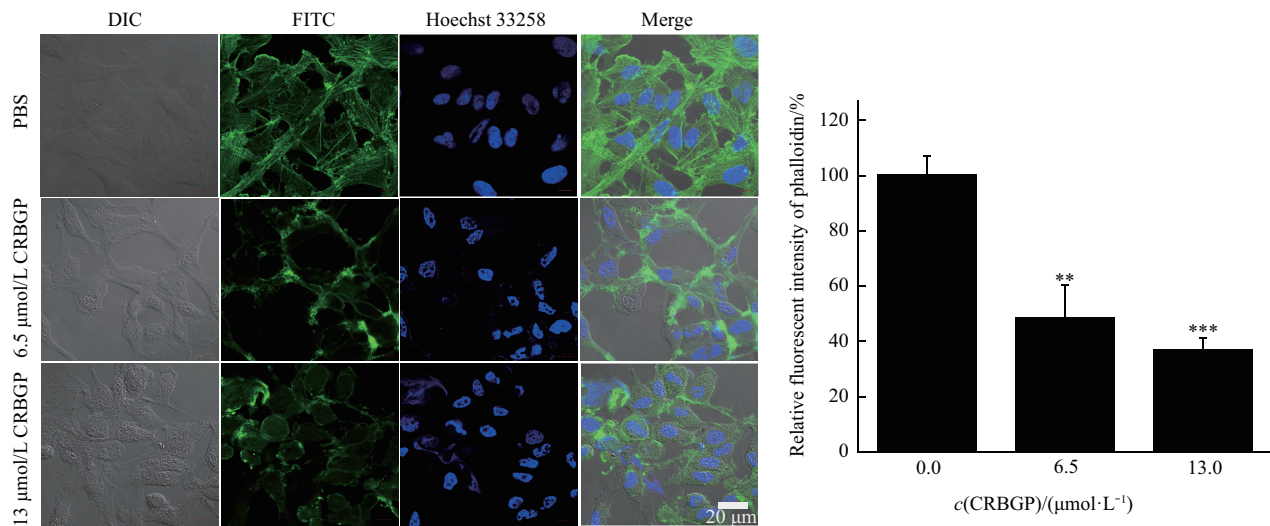


Fig. 3 CRBGP affected the cytoskeleton and nuclei of glioma U251 cells (630 \times magnification)

After treating with PBS, 6.5 and 13 $\mu\text{mol/L}$ CRBGP, the cytoskeleton and nuclei of U251 cells were labeled with FITC-phalloidin and Hoechst 33258 as mentioned in **Materials and methods**. The histogram showed the relative fluorescent intensity of phalloidin in the U251 cells treated with PBS, 6.5 and 13 $\mu\text{mol/L}$ CRBGP, respectively. The significant differences between the control and CRBGP groups were marked by asterisks (** $P < 0.01$; *** $P < 0.001$).

was analyzed by Western blot. As shown in Figure 4, CRBGP significantly elevated the BAX level, but decreased the BCL2 and Caspase 3 levels. Compared with the PBS group, 6.5 and 13 $\mu\text{mol/L}$ CRBGP increased BAX level by (1.33 \pm 0.25)-fold ($P < 0.01$) and (4.29 \pm 0.33)-fold ($P < 0.001$), reduced the BCL2 level to (57.1 \pm 3.4)% ($P < 0.01$) and (16.6 \pm 4.6)% ($P < 0.001$) of the control group, as well as increased the ratio of BAX/BCL2 by (3 \pm 0.27)-fold ($P < 0.01$) and (31 \pm 2.1)-fold ($P < 0.001$), respectively (Figure 4). And 13 $\mu\text{mol/L}$ CRBGP reduced the Caspase 3 level by (32 \pm 7)% ($P < 0.05$) while 6.5 $\mu\text{mol/L}$ CRBGP

seemed to have the opposite effect (Figure 4). Thus, CRBGP induced apoptosis in the U251 cells through a mitochondrial-dependent pathway mediated by BAX/BCL2 and Caspase 3.

2.4 The abilities of glioma U251 cells on adhesion, migration and invasion were reduced by CRBGP through FAK–AKT pathway

Based on the previous studies, glioma cells possess relatively higher mobility as they could migrate a distance of their cell diameter in just 5–10 min^[5]. More importantly, VGSCs were reported to be associated with the mobility of tumor cells^[20–22].

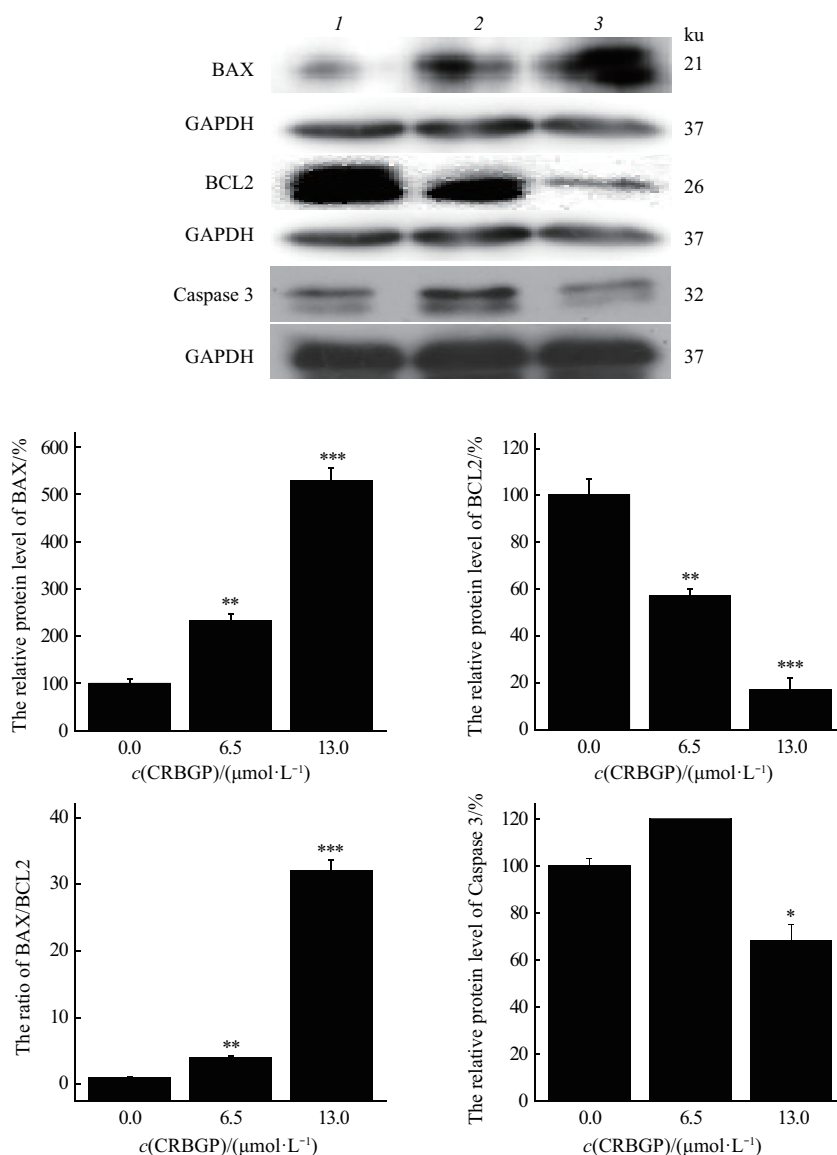


Fig. 4 CRBGP changed the concentration of apoptosis-related proteins in glioma U251 cells

After treating with PBS (lane 1), 6.5 (lane 2) and 13 $\mu\text{mol/L}$ CRBGP (lane 3), the level of apoptosis-related proteins including BAX, BCL2, and Caspase 3 was assayed by Western blots with GAPDH as an internal control. Gray values were obtained from FluorChem Q software and the histograms were drawn to indicate the change of the above proteins in the U251 cells which have been treated with PBS and CRBGP. The significant differences between the control and CRBGP groups were marked by asterisks (* $P < 0.05$; ** $P < 0.01$; *** $P < 0.001$).

Thus, we analyzed the effects of VGSCs inhibitor CRBGP on the mobility of glioma U251 cells. As shown in Figure 5, CRBGP inhibited the U251 cells' adhesion to the ECM proteins including collagen IV, fibronectin and laminin. The inhibitory ratios of 6.5 and 13 $\mu\text{mol/L}$ CRBGP on U251 cells' adhesion to collagen IV were (13 \pm 4)% and (78 \pm 2.5)% ($P < 0.001$), respectively; the inhibitory ratios of 6.5 and 13 $\mu\text{mol/L}$ CRBGP on U251 cells' adhesion to fibronectin were

(10 \pm 3)% and (50 \pm 3)% ($P < 0.001$), respectively; the inhibitory ratios of 6.5 and 13 $\mu\text{mol/L}$ CRBGP on U251 cells' adhesion to laminin were (37 \pm 2.5)% ($P < 0.001$) and (73 \pm 1.25)% ($P < 0.001$), respectively. In addition, the migration and invasion of the U251 cells were significantly inhibited in the presence of CRBGP (Figure 6, 7). CRBGP at 6.5 and 13 $\mu\text{mol/L}$ decreased the migrated percentage of the U251 cells by (38 \pm 1)% ($P < 0.001$) and (63 \pm 1.5)% ($P < 0.001$),

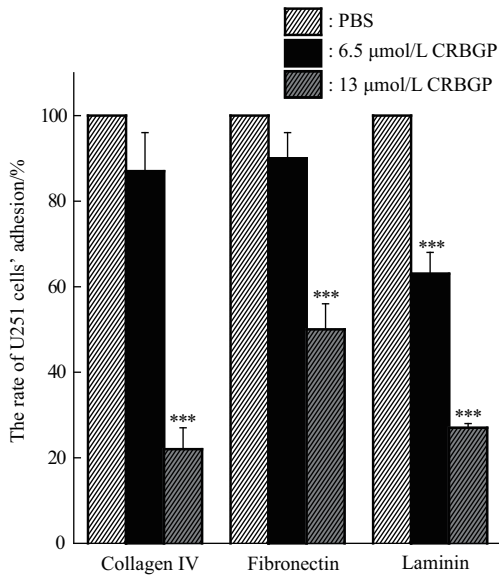


Fig. 5 CRBGP suppressed glioma U251 cells to adhere to collagen IV, fibronectin, and laminin, respectively

The significant differences of U251 cells' adhesion rate between the PBS and CRBGP-treated groups were indicated by asterisks (***) ($P < 0.001$).

respectively; while 6.5 and 13 μmol/L CRBGP decreased the invaded percentage of the U251 cells by (41±2.5)% ($P < 0.05$) and (72±2)% ($P < 0.01$), respectively. In order to further investigate the underlying mechanism of the inhibitory effects of CRBGP on the mobility of glioma U251 cells, Western blots were used to detect the content of signal molecules related to the migration and invasion of the U251 cells. As shown in Figure 8, the level of p-FAK was decreased in a dose-dependent manner. Compared with the PBS treating group, 6.5 and 13 μmol/L CRBGP decreased the level of p-FAK by (49.8±7.5)% ($P < 0.05$) and (66±5)% ($P < 0.01$), respectively. Also, CRBGP treatment could lead to the decrease of p-AKT level in the U251 cells (Figure 8). Compared with the PBS group, 6.5 and 13 μmol/L CRBGP decreased the level of p-AKT by (7±5)% and (82±3)% ($P < 0.001$), respectively (Figure 8). These data indicated that CRBGP inhibited the abilities of U251 cells on adhesion, migration and invasion by suppressing the activity of FAK-AKT pathway.

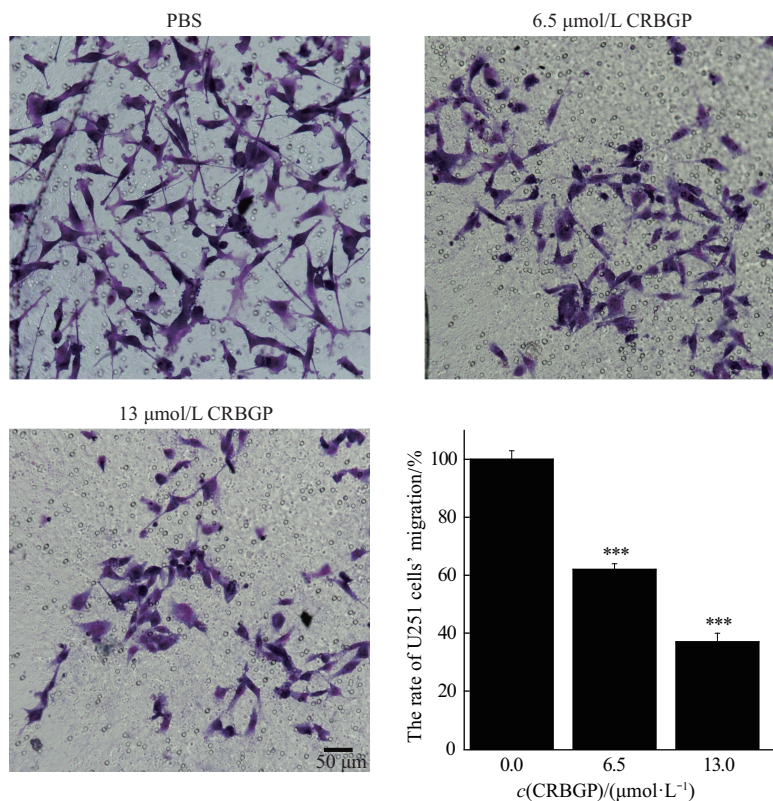


Fig. 6 CRBGP reduced the number of the migrated glioma U251 cells

Three fields in the U251 cells treated with PBS, 6.5 and 13 μmol/L CRBGP were randomly selected and captured to count the number of the migrated U251 cells through the microscope. Among the three fields, the representative graph on migration in each group was chosen and shown. The percentage of U251 cells' migration was calculated based on the number of the U251 cells in the mentioned fields, and the significant differences were shown by asterisks (***) ($P < 0.001$).

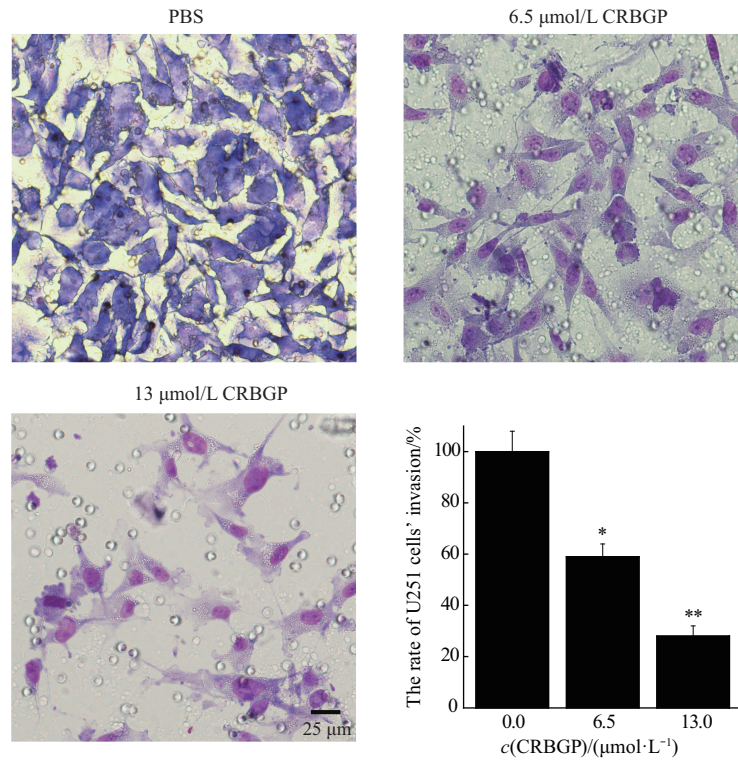


Fig. 7 CRBGP reduced the number of the invaded glioma U251 cells

Three fields in the U251 cells treated with PBS, 6.5 and 13 μmol/L CRBGP were randomly selected and captured to count the number of the invaded U251 cells through the microscope. Among the three fields, the representative graph on invasion in each group was chosen and shown. The percentage of U251 cells' invasion was calculated based on the number of the U251 cells in the mentioned fields, and the significant differences were shown by asterisks (* $P < 0.05$; ** $P < 0.01$).

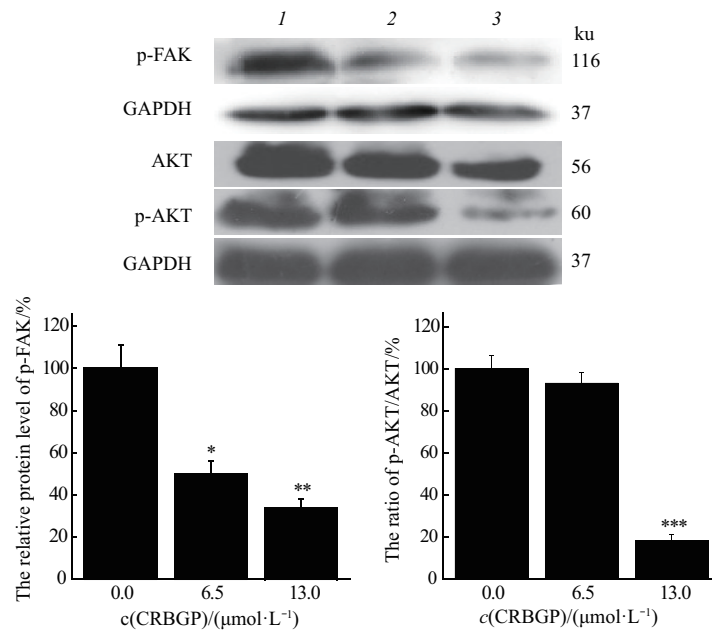


Fig. 8 CRBGP decreased the level of p-FAK and p-AKT in glioma U251 cells

After treating with PBS (lane 1), 6.5 (lane 2) and 13 μmol/L CRBGP (lane 3), the level of p-FAK, as well as p-AKT was analyzed by Western blots with GAPDH as an internal control. Gray values were obtained from FluorChem Q software and the histograms were drawn to indicate the change of the above proteins in the U251 cells which have been treated with PBS and CRBGP. The significant differences between the control and CRBGP groups were marked by asterisks (* $P < 0.05$; ** $P < 0.01$; *** $P < 0.001$).

2.5 CRBGP suppressed the release of inflammatory factor IL-6 from glioma U251 cells

Accumulating evidence showed that inflammation would promote the development of gliomas^[23-25]. As CRBGP was reported to possess anti-inflammatory property in our previous study^[26], whether CRBGP could also inhibit the activity of U251 cells through its regulation on inflammatory response? Therefore, the level of inflammatory factor IL-6 in the supernatant of the U251 cells treated with CRBGP was examined by ELISA. As shown in Figure 9, CRBGP was able to inhibit the U251 cells to release IL-6 in a dose-dependent manner. And the levels of IL-6 in the 6.5 and 13 $\mu\text{mol/L}$ CRBGP treating groups was respectively reduced to $(30.7 \pm 0.85)\%$ ($P < 0.01$) and $(18.8 \pm 2.4)\%$ ($P < 0.01$) of the control group (Figure 9). After stimulation with LPS from *Escherichia coli* (*E. coli*), the level of IL-6 in the supernatant of the U251 cells was increased dramatically, from (387.7 ± 40) ng/L in the unstimulated group to $(1\ 039.3 \pm 63)$ ng/L in the LPS-stimulated U251 cells (Figure 9). Although LPS was able to induce the release of IL-6 from the U251 cells, CRBGP still could effectively suppress the level of

IL-6 in the supernatant of the U251 cells. The inhibitory ratio of IL-6 release by 6.5 and 13 $\mu\text{mol/L}$ CRBGP were $(73.0 \pm 1.69)\%$ ($P < 0.01$) and $(88.2 \pm 0.66)\%$ ($P < 0.01$), respectively (Figure 9). Thus, the above results showed the CRBGP was able to inhibit the activity of U251 cells through its anti-inflammatory effect.

3 Discussion

In the present study, CRBGP was shown to suppress the proliferation of glioma U251 cells with an IC_{50} of 8.3 $\mu\text{mol/L}$, which was similar to the effect of CRBGP on cervical cancer HeLa cells^[16]. This meant that CRBGP which was identified as a VGSCs blocker might not only act on these two tumor cells, but also on the other tumor cells as long as the VGSCs are expressed. Different from HeLa cells, U251 cells are characterized with high infiltration ability^[4-5]. This might account for the difference of its IC_{50} between the HeLa cells and U251 cells. Previous studies have shown that the subtypes of α subunit of VGSCs in the primary cultures and biopsies of cervical cancer are Nav1.2, Nav1.4, Nav1.6, and Nav1.7^[27]. Also, Lopez-Charcas *et al.*^[28-29] further confirmed that HeLa cells might express a truncated isoform of Nav1.6; whereas U251 cells were reported to express the neonatal Nav1.6 (nNav1.6) in the nucleus, cytoplasm and membrane of the cells^[9]. nNav1.6 was proved to promote the proliferation, migration and invasion, as well as to prevent apoptosis in U251 cells^[9]. In addition, nNav1.6 which was firstly identified in human brain neuroblastoma NB-1 cells is an alternative splicing product from the *SCN5A* gene which is regarded as an oncogene and would finally result in the formation and progression of tumor cells^[9, 30-33]. Thus, the different subtypes of α subunit of VGSCs on HeLa and U251 cells might lead to the different responses of these two tumor cells induced by CRBGP.

Combining the confocal microscope observation and Western blot analysis, the anti-proliferative property of CRBGP on U251 cells would be attributed to apoptosis, which is similar to the effect of CRBGP on cervical cancer HeLa cells^[16]. Similarly, CRBGP also induced apoptosis in U251 cells in a mitochondrial-dependent manner as the content change of BAX, BCL2 and Caspase 3 was coincident with the rules of this way^[34-35].

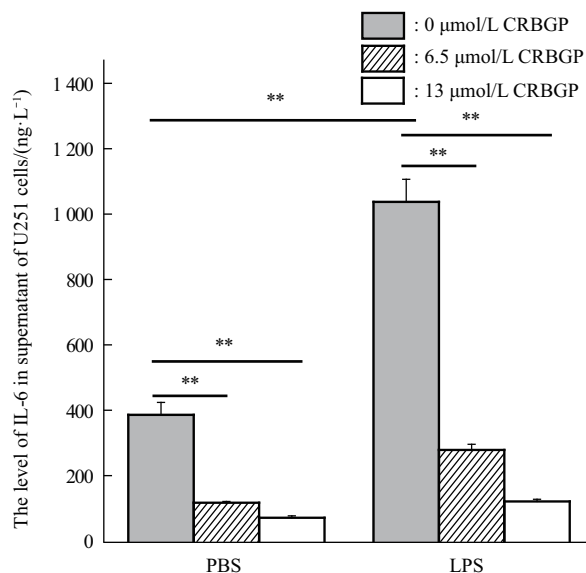


Fig. 9 CRBGP suppressed the release of IL-6 from the glioma U251 cells stimulated with the LPS originated from *E. coli*

The U251 cells were firstly stimulated with PBS and LPS, respectively. After 5 h, PBS, 6.5 and 13 $\mu\text{mol/L}$ CRBGP were respectively added into the above U251 cells. The concentration of IL-6 in the supernatant of the U251 cells was detected by ELISA. The significant differences were indicated with asterisks (** $P < 0.01$).

As we all know, inflammation is closely associated with the progression and metastasis of the tumors^[36]. To date, a great number of studies have shown that proinflammatory cytokine IL-6 was detected in the serum of pancreatic cancer patients, breast cancer patients, as well as glioma patients which might be potentially used as a prognostic marker in the future^[37-39]. Furthermore, IL-6 was reported to promote the occurrence and development of gliomas in glioma microenvironment^[23-25]. It is shown that CRBGP could significantly reduce the level of IL-6 in the supernatant of the U251 cells in a dose-dependent manner (Figure 9), suggesting that CRBGP might inhibit the glioma development through its anti-inflammatory property. This is coincident with our previous study in which recombinant CRBGP (also called as rLj-NIF) was shown to possess anti-inflammatory property as it was able to inhibit the activation, migration and adhesion of neutrophils^[26]. 2016, Zeuner and colleagues^[40] found that LPS originated from *E. coli* is capable of activating the MyD88-dependent signaling pathway through toll-like receptor 4 which locates at the membrane of the U251 cells to induce inflammatory responses. After translocation of the NF- κ B subunit p65, the activity of NF- κ B would be increased which would further promote the expression of its target genes and the release of IL-6^[40]. Subsequently, the released IL-6 could finally induce the proliferation of U251 cells^[40]. As shown in Figure 9, even if the U251 cells were pre-stimulated with LPS originated from *E. coli*, CRBGP still has the ability to inhibit the release of IL-6. This means that the anti-inflammatory characterization of CRBGP might be another reason to suppress the proliferation and mobility of U251 cells.

Although original studies identified VGSCs as transmembrane proteins which control the membrane potentials of neurons and muscle cells, recent studies found VGSCs can promote the metastasis of tumor cells mainly by their α and β subunits which would finally affect the adhesion, migration and invasion of the tumor cells^[20]. Actually, nNav1.5 was proved to promote the migration and invasion process of astrocytoma U251 cells^[9]. This means that CRBGP has suppressing activity on the mobility of U251 cells by its inhibitory effect on VGSCs. Furthermore, FAK, a non-receptor tyrosine kinase, was found to be up-regulated and activated in gliomas^[41]. To date, FAK

was known to affect the grade of gliomas as it could promote the proliferation, migration and invasion of the cells^[41-43]. According to the previous studies, the activated FAK can form complex with Src, and the Tyr 397 of FAK can directly bind to the SH2 domain of PI3K to activate PI3K. Subsequently, the activated PI3K would in turn activate AKT which regulates the cell growth and movement through the TSC2-mTOR-S6K pathway. Furthermore, PI3K can also participate in the Rac-JNK pathway to regulate the proliferation, differentiation and metastasis of tumor cells^[44]. In the present study, CRBGP could reduce the level of p-FAK and its downstream molecule p-AKT, suggested that CRBGP might inhibit the mobility of the glioma U251 cells through the FAK-AKT pathway. In addition, previous studies showed epidermal growth factor is up-regulated in a variety of tumor cells and is able to activate Ras-ERK signaling cascades to promote the expression of voltage-gated ion channels, which would promote tumor cell invasion^[45-47]. As CRBGP is a VGSCs blocker and was found to inhibit the mobility of the U251 cells, CRBGP might also affect the Ras-ERK signaling cascades. However, it requires further studies to clarify the question.

Similar to the effects of CRBGP on the HUVECs and Hela cells, CRBGP could repress the glioma U251 cells to attach to the same ECM proteins^[14, 16]. As both the α and β subunits of VGSCs could promote the cells to attach to the ECM proteins, the VGSCs modulating activity of CRBGP might be responsible for its inhibitory effect on the adhesion of the glioma U251 cells^[21-22].

Previous studies have shown that the rearrangement of the tumor cells' cytoskeleton is closely related to changes of the expression, localization and even function of ion channels. In tumor cells, ion channels interact with certain components of the cytoskeleton directly, which finally promote the metastasis of tumor cells^[48]. Also, the β 2 subunit of VGSCs was reported to interact with the adhesion molecules which would lead to the reorganization of the cytoskeleton and finally promote the metastasis of tumor cells. Furthermore, VGSCs were shown to affect the cytoskeleton by regulating the content of intracellular Ca^{2+} ^[49]. Thus, we speculated that CRBGP might also alter the F-actin organization in the U251 cells indirectly by affecting the VGSCs. However, further studies are still required to clarify this question and more novel drugs that

target gliomas are still welcomed^[50].

4 Conclusion

Taken together, CRBGP has the ability to inhibit the proliferation and mobility of the glioma U251 cells with the relatively higher infiltrative property through the FAK-AKT pathway (Figure 10). The anti-

proliferative effect of CRBGP on glioma U251 cells was mainly due to mitochondrial-dependent apoptosis and its anti-inflammatory activity. Furthermore, CRBGP may suppress glioma U251 cells to attach to ECM proteins, as well as their migration and infiltration through its VGSCs blocking activity, and its anti-inflammatory activity (Figure 10).

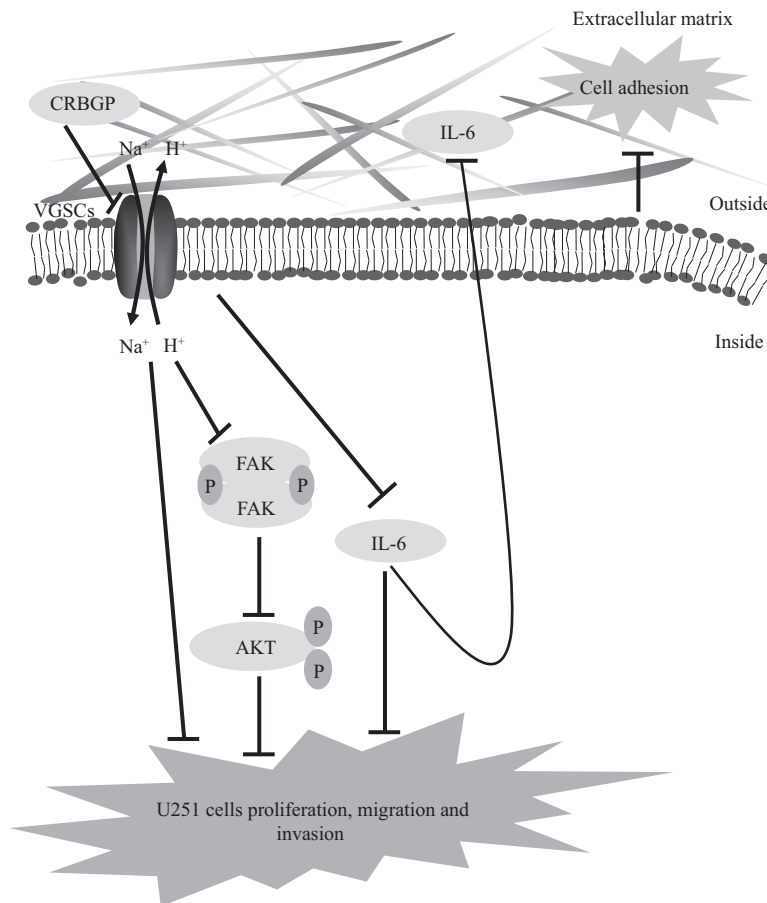


Fig. 10 The potential mechanisms of CRBGP on its inhibitory effects on the glioma U251 cells

CRBGP might target the VGSCs on the membrane of the U251 cells to block the U251 cells' proliferation and mobility as the activity of VGSCs could promote the proliferation and mobility of the U251 cells^[9]. In addition, CRBGP was also able to suppress the activation of FAK, a key factor to initiate the mobility of the tumor cells, and its downstream molecule AKT in U251 cells to suppress their adhesion, migration and invasion. Lastly, CRBGP would inhibit the activity of U251 cells by suppressing the release of IL-6, which was reported to promote the proliferation, survival, angiogenesis and immune escape of the tumor cells, probably due to its immune repression property^[51].

References

- [1] Van Meir E G, Hadjipanayis C G, Norden A D, *et al.* Exciting new advances in neuro-oncology: the avenue to a cure for malignant glioma. *CA Cancer J Clin*, 2010, **60**(3): 166-193
- [2] Qi L, Ding L, Wang S, *et al.* A network meta-analysis: the overall and progression-free survival of glioma patients treated by different chemotherapeutic interventions combined with radiation therapy (RT). *Oncotarget*, 2016, **7**(42): 69002-69013
- [3] Simonelli M, Persico P, Perrino M, *et al.* Checkpoint inhibitors as treatment for malignant gliomas: "a long way to the top". *Cancer Treat Rev*, 2018, **69**: 121-131
- [4] Ferrer V P, Neto V M, Mentlein R. Glioma infiltration and extracellular matrix: key players and modulators. *Glia*, 2018, **66**(8): 1542-1565
- [5] Khain E, Katakowski M, Charteris N, *et al.* Migration of adhesive

- glioma cells: front propagation and fingering. *Phys Rev E Stat Nonlin Soft Matter Phys*, 2012, **86**(1 Pt 1): 011904
- [6] Mesti T, Ocvirk J. Malignant gliomas: old and new systemic treatment approaches. *Radiol Oncol*, 2016, **50**(2): 129-138
- [7] Ghotme K A, Barreto G E, Echeverria V, *et al.* Gliomas: new perspectives in diagnosis, treatment and prognosis. *Curr Top Med Chem*, 2017, **17**(12): 1438-1447
- [8] Liu C A, Chang C Y, Hsueh K W, *et al.* Migration/invasion of malignant gliomas and implications for therapeutic treatment. *Int J Mol Sci*, 2018, **19**(4): 1115
- [9] Xing D, Wang J, Ou S, *et al.* Expression of neonatal Nav1.5 in human brain astrocytoma and its effect on proliferation, invasion and apoptosis of astrocytoma cells. *Oncol Rep*, 2014, **31**(6): 2692-2700
- [10] Zhang Y, Zhou L, Zhang J, *et al.* Suppression of chloride voltage-gated channel 3 expression increases sensitivity of human glioma U251 cells to cisplatin through lysosomal dysfunction. *Oncol Lett*, 2018, **16**(1): 835-842
- [11] Lepannetier S, Zanou N, Yerna X, *et al.* Sphingosine-1-phosphate-activated TRPC1 channel controls chemotaxis of glioblastoma cells. *Cell Calcium*, 2016, **60**(6): 373-383
- [12] Turner K L, Honasoge A, Robert S M, *et al.* A proinvasive role for the Ca²⁺-activated K⁺ channel KCa3.1 in malignant glioma. *Glia*, 2014, **62**(6): 971-981
- [13] Chi S, Xiao R, Li Q, *et al.* Suppression of neuronal excitability by the secretion of the lamprey (*Lampetra japonica*) provides a mechanism for its evolutionary stability. *Pflugers Arch*, 2009, **458**(3): 537-545
- [14] Jiang Q, Liu Y, Duan D, *et al.* Anti-angiogenic activities of CRBGP from buccal glands of lampreys (*Lampetra japonica*). *Biochimie*, 2016, **123**: 7-19
- [15] Jiang Q, Liu Y, Gou M, *et al.* Data for the inhibition effects of recombinant lamprey CRBGP on the tube formation of HUVECs and new blood vessel generation in CAM models. *Data Brief*, 2016, **6**: 661-667
- [16] Han J, Liu Y, Jiang Q, *et al.* Cysteine-rich buccal gland protein suppressed the proliferation, migration and invasion of hela cells through akt pathway. *IUBMB Life*, 2017, **69**(11): 856-866
- [17] Andrikopoulos P, Fraser S P, Patterson L, *et al.* Angiogenic functions of voltage-gated Na⁺ Channels in human endothelial cells: modulation of vascular endothelial growth factor (VEGF) signaling. *J Biol Chem*, 2011, **286**(19): 16846-16860
- [18] Pan H, Zhao Q, Zhan Y, *et al.* Expression and distribution of voltage-gated sodium channels in cervical cancer cells and its role in cell proliferation and invasion. *Chin J Clin Oncol*, 2012, **39**(4): 189-193
- [19] Xiao R, Li Q W, Perrett S, *et al.* Characterisation of the fibrinolytic properties of the buccal gland secretion from *Lampetra japonica*. *Biochimie*, 2007, **89**(3): 383-392
- [20] Patel F, Brackenbury W J. Dual roles of voltage-gated sodium channels in development and cancer. *Int J Dev Biol*, 2015, **59**(7-9): 357-366
- [21] Poffers M, Bühne N, Herzog C, *et al.* Sodium channel Nav1.3 is expressed by polymorphonuclear neutrophils during mouse heart and kidney ischemia *in vivo* and regulates adhesion, transmigration, and chemotaxis of human and mouse neutrophils *in vitro*. *Anesthesiology*, 2018, **128**(6): 1151-1166
- [22] Kruger L C, Isom L L. Voltage-gated Na⁺ channels: not just for conduction. *Cold Spring Harb Perspect Biol*, 2016, **8**(6): a029264
- [23] Chen W, Xia T, Wang D, *et al.* Human astrocytes secrete IL-6 to promote glioma migration and invasion through upregulation of cytomembrane MMP14. *Oncotarget*, 2016, **7**(38): 62425-62438
- [24] Weissenberger J, Loeffler S, Kappeler A, *et al.* IL-6 is required for glioma development in a mouse model. *Oncogene*, 2004, **23**(19): 3308-3316
- [25] Yeung Y T, McDonald K L, Grewal T, *et al.* Interleukins in glioblastoma pathophysiology: implications for therapy. *Br J Pharmacol*, 2013, **168**(3): 591-606
- [26] Xue Z, Bai J, Sun J, *et al.* Novel neutrophil inhibitory factor homologue in the buccal gland secretion of *Lampetra japonica*. *Biol Chem*, 2011, **392**(7): 609-616
- [27] Diaz D, Delgadillo D M, Hernández-Gallegos E, *et al.* Functional expression of voltage-gated sodium channels in primary cultures of human cervical cancer. *J Cell Physiol*, 2007, **210**(2): 469-478
- [28] Lopez-Charcas O, Espinosa A M, Alfaro A, *et al.* The invasiveness of human cervical cancer associated to the function of Na_v1.6 channels is mediated by MMP-2 activity. *Sci Rep*, 2018, **8**(1): 12995
- [29] Plummer N W, McBurney M W, Meisler M H. Alternative splicing of the sodium channel *SCN8A* predicts a truncated two-domain protein in fetal brain and non-neuronal cells. *J Biol Chem*, 1997, **272**(38): 24008-24015
- [30] Ou S W, Kameyama A, Hao L Y, *et al.* Tetrodotoxin-resistant Na⁺ channels in human neuroblastoma cells are encoded by new variants of Nav1.5/*SCN5A*. *Eur J Neurosci*, 2005, **22**(4): 793-801
- [31] Wang J, Ou S W, Wang Y J, *et al.* New variants of Nav1.5/*SCN5A* encode Na⁺ channels in the brain. *J Neurogenet*, 2008, **22**(1): 57-75
- [32] Brackenbury W J, Chioni A M, Diss J K, *et al.* The neonatal splice variant of Nav1.5 potentiates *in vitro* invasive behaviour of MDA-MB-231 human breast cancer cells. *Breast Cancer Res Treat*, 2007, **101**(2): 149-160
- [33] Yamaci R F, Fraser S P, Battaloglu E, *et al.* Neonatal Nav1.5 protein expression in normal adult human tissues and breast cancer. *Pathol Res Pract*, 2017, **213**(8): 900-907
- [34] Dai H, Meng X W, Kaufmann S H. Mitochondrial apoptosis and BH3 mimetics. *F1000Res*, 2016, **5**: 2804
- [35] Sarosiek K A, Letai A. Directly targeting the mitochondrial pathway of apoptosis for cancer therapy using BH3 mimetics: recent successes, current challenges and future promise. *FEBS J*, 2016, **283**(19): 3523-3533
- [36] Razidlo G L, Burton K M, McNiven M A. Interleukin-6 promotes pancreatic cancer cell migration by rapidly activating the small GTPase CDC42. *J Biol Chem*, 2018, **293**(28): 11143-11153
- [37] Breitbart W, Rosenfeld B, Tobias K, *et al.* Depression, cytokines,

- and pancreatic cancer. *Psychooncology*, 2014, **23**(3): 339-345
- [38] Kaur R P, Vasudeva K, Singla H, *et al.* Analysis of pro- and anti-inflammatory cytokine gene variants and serum cytokine levels as prognostic markers in breast cancer. *J Cell Physiol*, 2018, **233**(12): 9716-9723
- [39] Shan Y, He X, Song W, *et al.* Role of IL-6 in the invasiveness and prognosis of glioma. *Int J Clin Exp Med*, 2015, **8**(6): 9114-9120
- [40] Zeuner M T, Krüger C L, Volk K, *et al.* Biased signalling is an essential feature of TLR4 in glioma cells. *Biochim Biophys Acta*, 2016, **1863**(12): 3084-3095
- [41] Ding L, Sun X, You Y, *et al.* Expression of focal adhesion kinase and phosphorylated focal adhesion kinase in human gliomas is associated with unfavorable overall survival. *Transl Res*, 2010, **156**(1): 45-52
- [42] Natarajan M, Hecker T P, Gladson C L. FAK signaling in anaplastic astrocytoma and glioblastoma tumors. *Cancer J*, 2003, **9**(2): 126-133
- [43] Golubovskaya V M, Huang G, Ho B, *et al.* Pharmacologic blockade of FAK autophosphorylation decreases human glioblastoma tumor growth and synergizes with temozolomide. *Mol Cancer Ther*, 2013, **12**(2): 162-172
- [44] Teutschbein J, Scharlt M, Meierjohann S. Interaction of *Xiphophorus* and murine Fyn with focal adhesion kinase. *Comp Biochem Physiol C Toxicol Pharmacol*, 2009, **149**(2): 168-174
- [45] Martin S W, Butcher A J, Berrow N S, *et al.* Phosphorylation sites on calcium channel $\alpha 1$ and β subunits regulate ERK-dependent modulation of neuronal N-type calcium channels. *Cell Calcium*, 2006, **39**(3): 275-292
- [46] Hakariya T, Shida Y, Sakai H, *et al.* EGFR signaling pathway negatively regulates PSA expression and secretion *via* the PI3K-Akt pathway in LNCaP prostate cancer cells. *Biochem Biophys Res Commun*, 2006, **342**(1): 92-100
- [47] Campbell T M, Main M J, Fitzgerald E M. Functional expression of the voltage-gated Na^+ -channel $\text{Na}_v 1.7$ is necessary for EGF-mediated invasion in human non-small cell lung cancer cells. *J Cell Sci*, 2013, **126**(Pt 21): 4939-4949
- [48] Rodat-Despoix L, Chamlali M, Ouadid-Ahidouch H. Ion channels as key partners of cytoskeleton in cancer disease. *Biochim Biophys Acta Rev Cancer*, 2021, **1876**(2): 188627
- [49] Fraser S P, Salvador V, Manning E A, *et al.* Contribution of functional voltage-gated Na^+ channel expression to cell behaviors involved in the metastatic cascade in rat prostate cancer: I. lateral motility. *J Cell Physiol*, 2003, **195**(3): 479-487
- [50] Zhang Y, Yang Y, Ye J, *et al.* Construction of chlorogenic acid-containing liposomes with prolonged antitumor immunity based on T cell regulation. *Sci China Life Sci*, 2021, **64**(7): 1097-1115
- [51] Naugler W E, Karin M. The wolf in sheep's clothing: the role of interleukin-6 in immunity, inflammation and cancer. *Trends Mol Med*, 2008, **14**(3): 109-119

CRBGP通过抑制FAK-AKT通路和白介素-6的 分泌抑制胶质瘤U251细胞的活性*

韩健美 李嘉阳 巴月 周蓉 李双娇 肖蓉**

(辽宁师范大学生命科学学院, 大连 116081)

摘要 目的 电压门控钠通道 (voltage-gated sodium channels, VGSCs) 表达于胶质瘤U251细胞, 并影响U251细胞的增殖、侵袭和凋亡。富含半胱氨酸的颊腺蛋白 (cysteine-rich buccal gland protein, CRBGP) 是一种从日本七鳃鳗颊腺中分离出来的VGSCs阻断剂。本文旨在探究CRBGP是否因具有VGSCs阻断功能从而能够抑制U251细胞的活性。**方法** 首先采用MTT法检测了CRBGP对U251细胞增殖的作用, 并分别利用莱特-吉姆萨、FITC-phalloidin和Hoechst 33258染色法观察CRBGP处理后U251细胞的形态、细胞骨架和细胞核。细胞外基质蛋白如IV型胶原蛋白、纤连蛋白和层黏连蛋白用于检测CRBGP对U251细胞黏附的影响。此外, 本文采用transwell法检测CRBGP处理后U251细胞的迁移和侵袭能力, 并通过Western blot方法探讨CRBGP诱导U251细胞凋亡并抑制其运动的内在机理。最后, 通过酶联免疫吸附测定法检测CRBGP对U251细胞的抑炎效果。**结果** CRBGP通过线粒体依赖途径诱导U251细胞凋亡, 阻断促炎因子白介素-6的释放, 从而抑制U251细胞增殖。同时, CRBGP对VGSCs的阻断作用和抗炎活性有助于其抑制U251细胞的黏附、迁移和侵袭。最后, CRBGP通过抑制FAK-AKT信号通路影响U251细胞的增殖和运动。**结论** CRBGP可能因具有VGSCs抑制特性而表现出抗肿瘤活性, 为VGSCs在胶质瘤中的作用提供了依据。

关键词 胶质瘤, U251细胞, 电压门控钠通道, 富含半胱氨酸的颊腺蛋白, 白介素-6

中图分类号 Q291, Q26

DOI: 10.16476/j.pibb.2021.0359

* 国家自然科学基金 (31301880) 和辽宁省自然科学基金 (20180550829) 资助项目。

** 通讯联系人。

Tel: 0411-85992862, E-mail: xiaorong_lnu@126.com

收稿日期: 2021-11-23, 接受日期: 2021-12-02